Eur. Phys. J. A **16**, 423–435 (2003)
DOI 10.1140/epja/i2002-10114-9

THE EUROPEAN PHYSICAL JOURNAL A

Pre-equilibrium dipole strength in charge asymmetric peripheral heavy-ion reactions

D. Pierroutsakou[1,a], M. Di Toro[2,3], F. Amorini[2,3], V. Baran[3,4], A. Boiano[1], A. De Rosa[1,5], A. D'Onofrio[6,1], G. Inglima[1,5], M. La Commara[1,5], A. Ordine[1], N. Pellegriti[2,3], F. Rizzo[2,3], V. Roca[1,5], M. Romoli[1], M. Sandoli[1,5], M. Trotta[1,5,b], and S. Tudisco[2,3]

[1] INFN, Sezione di Napoli, Napoli, Italy
[2] Università di Catania, Dipartimento di Fisica, Catania, Italy
[3] INFN, Laboratorio Nazionale del Sud, Catania, Italy
[4] NIPNE-HH and Bucharest University, Romania
[5] Università di Napoli "Federico II", Dipartimento di Scienze Fisiche, Napoli, Italy
[6] Seconda Università di Napoli, Dipartimento di Scienze Ambientali, Napoli, Italy

Received: 26 September 2002 / Revised version: 11 November 2002 /
Published online: 6 March 2003 –
Communicated by C. Signorini

Abstract. We report on the results obtained from the study of the ^{32}S + ^{64}Ni and ^{32}S + ^{58}Ni peripheral reactions at incident energies $E_{\rm lab}$ = 288 MeV and $E_{\rm lab}$ = 320 MeV, respectively. High-energy γ-rays were detected in an array of 8 seven-pack BaF_2 clusters. Coincidence with complex fragments detected in 12 three-stage telescopes ensured the selection of peripheral reaction events. All of the relevant reaction parameters were kept constant with the exception of the different initial dipole moment caused by the different entrance channel charge asymmetry. While for quasi-elastic events no N/Z effect was observed in the differential γ-ray multiplicities of the two reactions, for deep-inelastic events a larger dipole γ-ray emission occurs during the more N/Z asymmetric reaction. A theoretical interpretation based on a collective Bremsstrahlung analysis of the reaction dynamics is presented.

PACS. 25.70.-z Low and intermediate energy heavy-ion reactions – 24.30.Cz Giant resonances – 23.20.-g Electromagnetic transitions – 25.70.Lm Strongly damped collisions

1 Introduction

Recently, a large interest has been devoted to the study of the prompt dipole γ-ray emission associated with the charge equilibration in heavy-ion collisions between partners with different N/Z ratios. Various theoretical works [1–4] predict that the dipole γ-ray emission in fusion reactions should depend on the N/Z ratio difference between the colliding ions and consequently on their initial dipole moment:

$$D(t=0) = \frac{NZ}{A}\left|\overrightarrow{R_Z}(t=0) - \overrightarrow{R_N}(t=0)\right| = \frac{R_p + R_t}{A} Z_p Z_t \left|\left(\frac{N}{Z}\right)_t - \left(\frac{N}{Z}\right)_p\right|$$

with $\overrightarrow{R_Z}$ and $\overrightarrow{R_N}$ the center of mass of protons and of neutrons, respectively, while R_p and R_t are the projectile and target radii.

The process of dipole strength excitation in the case of a net dipole moment in the entrance channel is different from the thermal excitation of the dipole vibration occuring in hot compound nuclei.

Experimentally, by studying fusion reactions differing in the entrance channel charge asymmetry, an excess of γ-rays emitted during the more N/Z asymmetric collision was observed [5–7]. This excess can be considered as indicative of pre-equilibrium dipole strength excitation.

Although theoretical works treating with the prompt dipole γ-ray emission are concentrated mainly on central heavy-ion collisions, in several experimental works [8–10], where N/Z asymmetric deep-inelastic heavy-ion collisions were studied, it was shown that dipole γ-rays are emitted not only by the excited complex fragments created during the collisions but also from the composite system before fragmentation. In [11], by considering the results of [8–10], it was indicated for the first time that the dipole γ-ray emission from the dinucleus increases with the entrance channel charge asymmetry.

The hypothesis of pre-equilibrium dipole strength excitation in N/Z asymmetric peripheral heavy-ion collisions

[a] e-mail: pierroutsakou@na.infn.it
[b] *Present address*: INFN, Laboratori Nazionali di Legnaro, Padova, Italy.

has been studied recently from a theoretical point of view in [12,13] with results in good agreement with the experimental findings of [8,10]. According to [13] an important part of the dipole γ-ray emission from the intermediate system created in the ^{32}S + ^{74}Ge deep-inelastic reaction is associated with the charge equilibration process between the colliding ions. It is predicted [13–15] and confirmed experimentally [10] that the dipole strength excited in such an intermediate system is shifted towards lower energies because of the high deformation of the emitting source.

Therefore, it seems reasonable to expect, also for the dipole strength excited in the intermediate system of peripheral heavy-ion collisions, a dependence on the entrance channel charge asymmetry. With the aim to investigate this hypothesis explicitly, two reactions have been performed: ^{32}S + ^{58}Ni and ^{32}S + ^{64}Ni at $E_{\rm lab}$ = 320 and 288 MeV, respectively, where the initial dipole moment changes from 3 fm for the almost N/Z symmetric system ^{32}S + ^{58}Ni to 11.46 fm for the asymmetric one ^{32}S + ^{64}Ni [16]. The other relevant reaction parameters such as the grazing angle, the grazing angular momentum and the Coulomb barrier were kept constant. The total excitation energy to be shared between the primary complex fragments, in the hypothesis of pre-equilibrium particle emission, was managed to be equal by choosing the appropriate region in the laboratory kinetic energy spectrum of the detected light fragment. It has to be noticed that the above quantities can be considered equal for both reactions within the analysis uncertainties (see sect. 4).

The present paper is organized as follows: in sect. 2 the experimental techniques are discussed, while in sect. 3 the differential γ-ray multiplicities associated with the two reactions for different degrees of dissipation are presented. In sect. 4, in order to isolate the γ-ray emission from the composite system, the γ-ray spectra originating in the statistical decay of the primary complex fragments are calculated by using a statistical model code. In sect. 5, calculations, based on a classical Bremsstrahlung approach, of the composite system dipole γ-ray emission are presented and compared with the present experimental outcome. Finally, the conclusions are given in sect. 6.

2 Experimental methods

The reactions were performed by using the pulsed beam of ^{32}S provided by the superconducting heavy-ion linear accelerator of the LNL (Laboratori Nazionali di Legnaro, Padova, Italy), impinging on 380 μg/cm^2 and 420 μg/cm^2 thick ^{64}Ni and ^{58}Ni self-supporting targets, respectively. The beam consisted of $\sim$ 2 ns wide bunches with a 200 ns separation. The beam intensity was measured in a Faraday cup shielded with lead and paraffin to reduce the background due to γ-rays and neutrons.

The γ-rays were detected by using 8 seven-pack clusters of BaF_2 scintillators of the TAPS standard situated at 28 cm from the target and at the following (θ, ϕ) angles with respect to the beam direction taken to coincide with the Oz-axis: (90°, 45°), (70°, 0°), (120°, 0°), (90°, 90°), (155°, 180°), (75°, 180°), (115 °, 180°), (90°, 135°). The total solid angle covered by the BaF_2 detectors was 17% of 4π sr. The BaF_2 clusters were surrounded by a 3 mm thick lead shield which reduced the counting rate due to the low-energy γ-rays ($E_\gamma \leq$1 MeV) to 50% and stopped the charged particles.

In this work, also the data of another experiment, where the ^{32}S + ^{58}Ni reaction was studied at an incident energy of 320 MeV, are considered to increase the statistics. In that run, performed at the LNL, three seven-pack clusters of BaF_2 scintillators were situated at 28 cm from the target and at the following (θ, ϕ) angles: (90°, 45°), (90°, 90°) and (90°, 135°). The other experimental conditions remained identical as previously. Then, the data collected with the BaF_2 scintillators situated at θ = 90° with respect to the beam direction of both experiments concerning the ^{32}S + ^{58}Ni reaction are included in the next section.

The reaction products were detected and charge identified by means of an array of 12 three-stage detectors each consisting of a gas ionization chamber, a silicon detector and a CsI(Tl) scintillator. These detectors were described in detail in [17]. The fragment detectors were placed at 35 cm from the target in the forward hemisphere with respect to the beam direction, covering the angular range between 11° and 37° and including the laboratory grazing angle $\theta_{\rm gr}$ = 14°. Their total solid angle was 0.144 sr.

Single peripheral events, where a particle detector was hit, together with coincidence events between a particle detector and at least one fired BaF_2 scintillator were collected during the experiment. A coincidence event was accepted if the deposited energy in a BaF_2 cluster was greater than $\sim$ 5 MeV. The threshold of the BaF_2 scintillators was set at $\sim$ 100 keV. The coincidence request eliminated any cosmic-ray contamination of the γ-ray spectra.

The discrimination between γ-rays and neutrons was performed by means of the measurement of the time of flight relative to the beam burst.

The energy calibration of the γ-ray detectors was obtained by using the sources of ^{60}Co, ^{88}Y and the composite sources of ^{241}Am + ^{9}Be and of ^{238}Pu + ^{13}C. The time stability of the energy calibration was verified during the experiment by monitoring the stability of the peak corresponding to a radioactive source. The energy calibration of the Si detectors was performed by using the elastic scattering of ^{32}S on various targets and the punch-through of the α-particles, while the energy calibration of the ionization chamber was performed by changing the gas pressure.

3 Ingredients and results of the analysis

In order to study the γ-ray energy spectra for peripheral events, in the off-line analysis only γ-rays in coincidence with secondary light fragments having atomic numbers from 10 to 18 were considered. During the experiment, the laboratory kinetic energy and the atomic number of the secondary light fragments were obtained. In fig. 1 the laboratory kinetic energy spectrum of the secondary fragments having atomic number Z = 16 emitted at θ = 19° during the ^{32}S + ^{64}Ni (upper panel) and the ^{32}S + ^{58}Ni

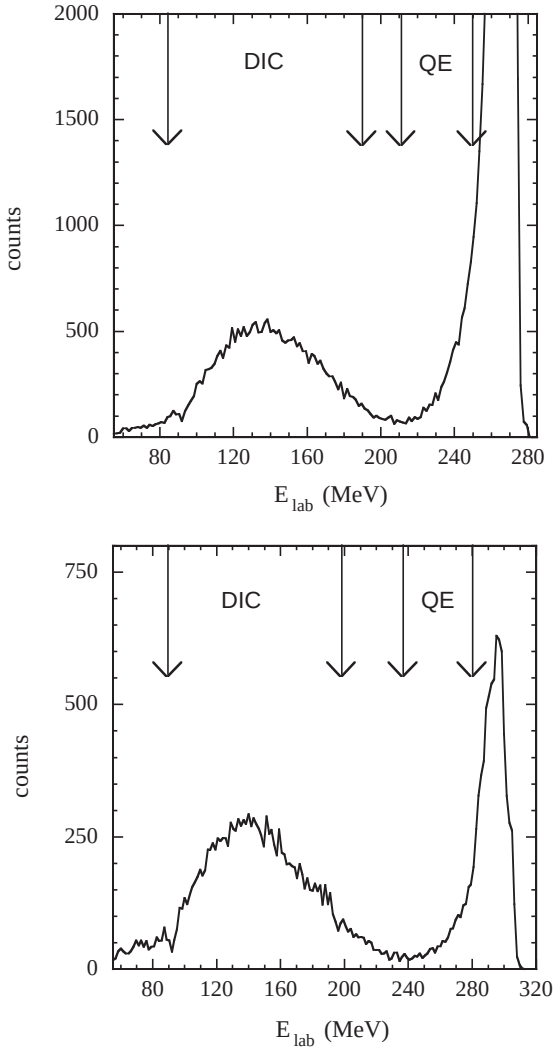

Fig. 1. Laboratory kinetic energy spectrum of the $Z = 16$ secondary fragments emitted at $\theta = 19°$ for the $^{32}S + ^{64}Ni$ (upper panel) and the $^{32}S + ^{58}Ni$ (lower panel) reaction. The arrows on the left hand side of the figure delimit deep-inelastic events, while those on the right hand side quasi-elastic events.

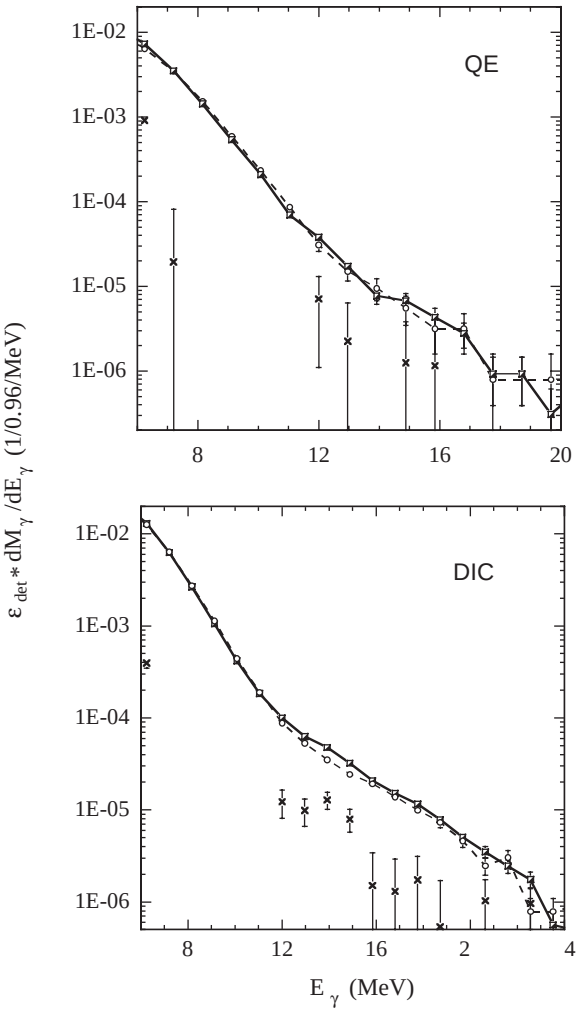

Fig. 2. Experimental γ-ray spectrum of the $^{32}S + ^{64}Ni$ (solid lines) and of the $^{32}S + ^{58}Ni$ (dashed lines) reaction for quasi-elastic (upper panel) and deep-inelastic (lower panel) events. The crosses represent the difference between the γ-ray spectra associated with the two reactions.

(lower panel) reaction is reported. These energy spectra have the shape typical of dissipative events with kinetic energy up to the quasi-elastic peak.

In peripheral collisions one is able to follow the evolution of the dipole strength excitation with the degree of kinetic energy dissipation or with the composite system excitation energy and lifetime by selecting different zones in the laboratory kinetic energy spectrum of the detected secondary light fragments. In the present analysis two different zones are considered. The first zone is related to fast quasi-elastic events (region between the arrows on the right hand side of fig. 1) characterized by a small dissipation of kinetic energy and a small nucleon transfer, while the second one (region between the arrows on the left hand side of fig. 1) is related to deep-inelastic events corresponding to slower reactions and larger energy dissipation.

As laboratory kinetic energy of all the secondary light fragments with the same atomic number, hitting each particle detector, was assumed the centroid of the considered region of their laboratory energy spectra. The center-of-mass kinetic energy of the primary light fragment was determined from the one of the detected ejectile by taking into account particle evaporation. The center-of-mass kinetic energy of the corresponding primary heavy fragment was then deduced in the hypothesis of a binary reaction. Finally, the center-of-mass kinetic energy in the exit channel for each fragmentation was inferred from that obtained with each particle detector by taking into account the detector experimental weight.

The total excitation energy shared between the primary fragments for each fragmentation can be written as

$$E^* = E_{\rm in} + Q_{\rm gg} - E_{\rm out}\,, \qquad (1)$$

where $E_{\rm in}$ and $E_{\rm out}$ are the center-of-mass kinetic energies in the reaction entrance and exit channels and $Q_{\rm gg}$ is the

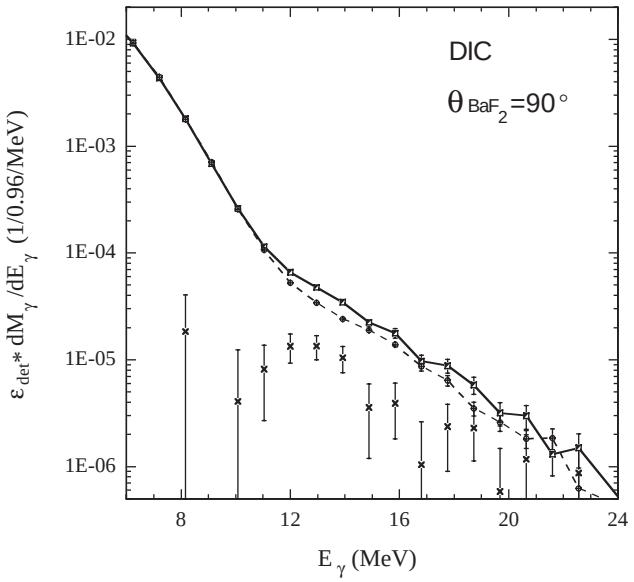

Fig. 3. Experimental γ-ray spectrum of the ^{32}S + ^{64}Ni (solid line) and of the ^{32}S + ^{58}Ni (dashed line) reaction obtained with BaF_2 scintillators situated at $\theta = 90^\circ$ with respect to the beam direction for deep-inelastic events. The crosses represent the difference between the γ-ray spectra associated with the two reactions.

ground-state Q value. In the case of pre-equilibrium light particle emission, the total excitation energy decreases from the value of eq. (1) by an amount ΔE taken away from the pre-equilibrium particles (see sect. 4).

In fig. 2 is reported the exclusive differential γ-ray multiplicity associated with the ^{32}S + ^{64}Ni (solid line) and the ^{32}S + ^{58}Ni (dashed line) reaction, for different energy dissipations. These spectra were obtained with all the γ-ray and particle detectors and are presented in the laboratory reference frame. $\varepsilon_{\rm det}$ is the efficiency of the experimental apparatus. In the upper panel of the figure the spectra for quasi-elastic reactions are presented, while in the lower one the spectra related with more dissipative collisions are shown (see the corresponding regions in fig. 1).

In the quasi-elastic and deep-inelastic case of fig. 2 the spectra correspond to the same average total excitation energy shared between the primary complex fragments for both reactions. The average total excitation energy was found to be $\sim$ 45 MeV for the quasi-elastic events and $\sim$ 110 MeV for the deep-inelastic ones by taking into account the pre-equilibrium emission of light particles as described in sect. 4. In the same figure, the crosses represent the difference between the experimental differential γ-ray multiplicities associated with the two reactions. From fig. 2 one can see that the differential γ-ray multiplicities corresponding to fast quasi-elastic events of the two reactions are identical within the error bars in the whole energy region of interest (upper panel of fig. 2) while for deep-inelastic events (lower panel of the same figure) a difference appears in the range E_γ = 10–16 MeV with a larger dipole γ-ray emission during the more N/Z asymmetric reaction.

In fig. 3 the cumulative experimental differential γ-ray multiplicity of the ^{32}S + ^{64}Ni (solid line) and the ^{32}S+^{58}Ni (dashed line) reaction obtained with the BaF_2 scintillators at $\theta = 90^\circ$ with respect to the beam direction together with their difference (crosses) are presented for deep-inelastic collisions. In this case as well, a clear difference between the data can be seen in the same energy range.

From the above, it seems that for quasi-elastic collisions, there is no difference within the error bars in the dipole γ-ray emission between the two reactions independently of their entrance channel charge asymmetry. However, by going towards slower, more dissipative events, there are more dipole γ-rays emitted in the more N/Z asymmetric reaction. The fact that for quasi-elastic reactions no N/Z effect was observed in the data can be attributed to the very short lifetime of the dinucleus ($t_0 \sim 10^{-22}$ s) as fragmentation occurs before complete relaxation of the charge degree of freedom between the colliding ions.

4 Evaluation of the complex fragment statistical γ-decay

The γ-rays detected in coincidence with the complex fragments originate in the γ-decay of the dinucleus before fragmentation as shown in [8–10] and in the statistical γ-decay of the fragments. Before attributing the difference between the γ-ray multiplicities associated with the two reactions to the difference of the respective dinucleus γ-decay, one has to evaluate and subtract from the experimental γ-ray spectra the statistical γ-ray spectra of the complex fragments emitted during the collisions.

In the following, only deep-inelastic events will be considered since only in this case a difference between the data was observed.

The excited complex fragments can be treated as completely equilibrated nuclei and their γ-ray spectrum can be calculated by using the statistical code CASCADE [18].

In this work, we recall briefly the main ingredients of the statistical model calculations since a detailed description of such calculations can be found in [10]. In the hypothesis of a binary fragmentation and of no pre-equilibrium particle emission, the masses of the primary complex fragments in coincidence with the considered experimental γ-ray spectrum are assumed to be roughly equal to those of the entrance channel. Then, we limit ourselves to calculate the statistical γ-ray spectrum of the most probable fragmentation, *i.e.* of S-like and Ni-like fragments.

For the present incident energies, $L_{\rm gr} = 127\hbar$, $L_{\rm cf} = 62\hbar$ for the ^{32}S + ^{64}Ni reaction and $L_{\rm gr} = 129\hbar$, $L_{\rm cf} = 59\hbar$ for the ^{32}S + ^{58}Ni reaction, with $L_{\rm gr}$ and $L_{\rm cf}$ the grazing angular momentum and the critical angular momentum for fusion, respectively.

The entrance channel angular momentum $\hbar L_{\rm i}$ was

$$\hbar L_{\rm i} = \hbar \left[L_{\rm cf} + 0.66 \left(L_{\rm gr} - L_{\rm cf} \right) \right] . \qquad (2)$$

According to the above relation $\hbar L_{\rm i}$ was $105\hbar$ for both reactions. The angular momentum $\hbar L_{\rm f}$ transferred to the

Table 1. Parameters used in the CASCADE code for the calculation of the complex fragment statistical γ-ray spectra in the hypothesis of no pre-equilibrium light particle emission.

Nucleus	E^* (MeV)	Spin ($\hbar$)	$E_{\rm GDR}$ (MeV)	$\Gamma_{\rm GDR}$ (MeV)	$S_{\rm GDR}$ (TRKSR)	a (MeV^{-1})
^{32}S	49	8	20	13	1	$A/8$
^{64}Ni	86	21	16.5	12	1	$A/8$
^{58}Ni	92	21	17	12	1	$A/8$

exit channel was obtained according to the sticking model which is appropriate for deep-inelastic events. The partition of the total dissipated angular momentum, $\hbar(L_{\rm i}-L_{\rm f})$, between the fragments was performed according to their moment of inertia.

The composite system moment of inertia at the scission point was calculated in the same way as in [10]. The total excitation energy shared between the primary fragments in the assumption of a binary reaction and of no pre-equilibrium light particle emission was determined as described in sect. 3. The total excitation energy sharing among the primary fragments was done proportionally to their masses according to a thermal equilibrium hypothesis at the fragmentation moment which is reasonable in the case of deep-inelastic events. The corresponding excitation energies and spins of the primary complex fragments emitted in the two reactions are listed in table 1.

For the projectile-like fragment an isospin dependent version of CASCADE [18] was used, while for the target-like fragment the usual isospin independent version was considered sufficient to describe its statistical γ-decay. To our knowledge, there is no experimental information on the GDR parameters in the ^{58}Ni and the ^{64}Ni compound nuclei formed at the same initial conditions as in the present work, *i.e.*, the same excitation energy and the same spin. Besides the data referring to the GDR built on the ground state of ^{58}Ni and the ^{60}Ni [19], there are data concerning the GDR decay of the hot equilibrated nuclei ^{63}Cu [20] and ^{59}Cu [21], formed at lower excitation energy, $E^* = 77.4$ MeV, than that of the present case and spin extending up to $J_{\rm crit} = 35\hbar$ and $J_{\rm crit} = 38\hbar$, respectively. Then, for the calculation of the statistical γ-ray spectra of the ^{58}Ni and the ^{64}Ni nuclei, the GDR centroid energy and the GDR strength were assumed to be equal within the errors to those quoted in [20,21], while the value of the GDR width for both the ^{58}Ni and the ^{64}Ni nuclei was taken to be intermediate between the values derived in [20,21]. However, the results of the analysis do not change by modifying the GDR parameters within ± 0.5 MeV for the centroid energy, ± 1 MeV for the width and ± 0.1 for the strength. The parameters used in the statistical model calculations are presented in table 1.

The theoretical γ-ray spectra were folded by the experimental set-up response function by using the code GEANT3 [22]. The Doppler shift correction due to the velocity of the fragments in the laboratory reference frame was also considered as described in [10].

The dominant mechanism which feeds the γ-ray spectra at energies larger than 20 MeV should be the nucleon-

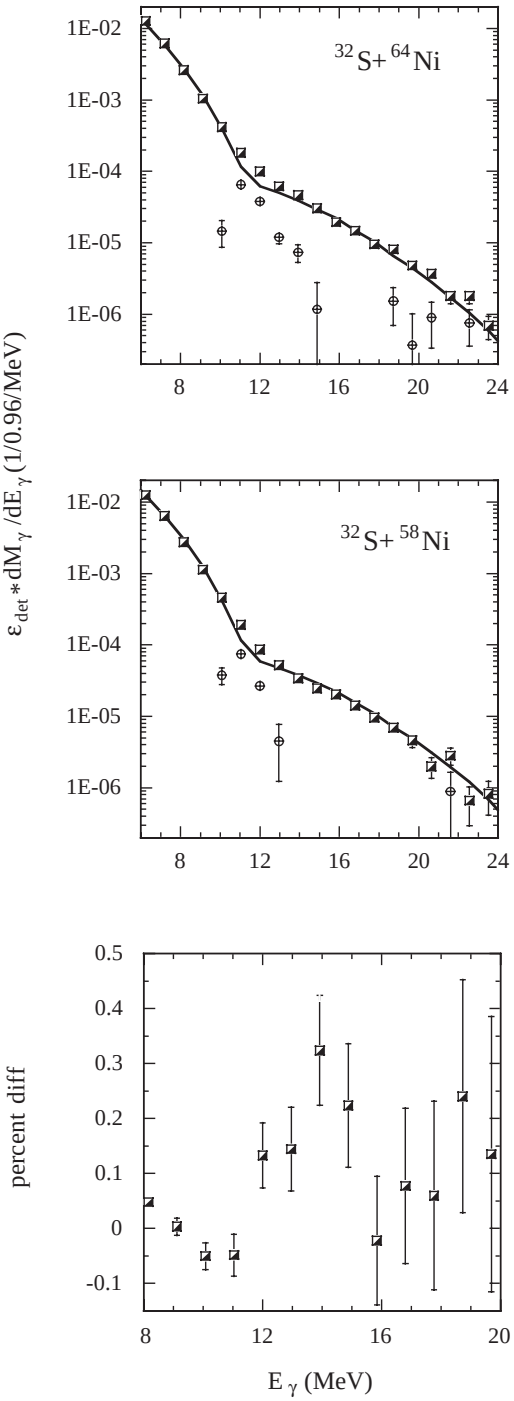

Fig. 4. Upper panel: experimental γ-ray spectrum of the ^{32}S + ^{64}Ni (squares) reaction, statistical γ-ray spectrum of the fragments (solid line) in the hypothesis of no pre-equilibrium particle emission and difference between the experimental and the statistical γ-ray spectrum (circles) representing the dinucleus γ-ray spectrum. The theoretical spectra are Doppler corrected and folded with the experimental set-up response function. Furthermore, they are divided by a factor of 1.8. Data and theoretical calculations are displayed in the laboratory reference frame. Middle panel: The same as in the upper panel for the ^{32}S + ^{58}Ni reaction. Lower panel: percent difference between the dinucleus γ-ray spectra associated with the two reactions (see text).

Table 2. Parameters used in the CASCADE code for the calculation of the complex fragment statistical γ-ray spectra in the hypothesis of pre-equilibrium emission of 2 nucleons.

Nucleus	E^* (MeV)	Spin ($\hbar$)	$E_{\rm GDR}$ (MeV)	$\Gamma_{\rm GDR}$ (MeV)	$S_{\rm GDR}$ (TRKSR)	a (MeV^{-1})
^{32}S	40	8	20	13	1	$A/8$
^{62}Co	68	21	17.8	11	1	$A/9$
^{56}Co	70	21	17.8	11	0.9	$A/9$

nucleon Bremsstrahlung [23]. At the present incident energy it represents no more than 15% of the γ-ray cross-section at $E_\gamma = 20$ MeV. As it affects in a small way the energy region between 10 and 18 MeV, its contribution was neglected in the analysis.

In order to reproduce the absolute value of the experimental γ-ray spectra the theoretical ones were normalized by dividing them by a factor of 1.8 for both reactions.

Experimental and theoretical γ-ray spectra are presented in fig. 4. In the upper and middle panel of the figure the squares correspond to the experimental γ-ray spectra of the ^{32}S + ^{64}Ni and ^{32}S + ^{58}Ni reaction, respectively, while the solid lines are the relative theoretical γ-ray spectra of the fragments. Both data and calculations are displayed in the laboratory reference frame. From fig. 4, one can see that the theoretical γ-ray spectra reproduce well the experimental ones associated with the two reactions at both low and high energies. However, as stated in [8–10], the statistical γ-decay of the complex fragments underpredicts the experimental γ-ray multiplicity in the energy range from ∼10 to ∼18 MeV. The difference between the experimental and the theoretical γ-ray multiplicity corresponds to the γ-ray emission from the dinucleus before fragmentation (circles of the upper and middle panel of fig. 4). In the lower panel of the same figure the percent difference is presented which corresponds to the difference between the γ-ray spectra associated with the dinucleus in the two reactions divided by the experimental γ-ray spectrum of the ^{32}S + ^{58}Ni reaction. The percent difference can be written:

$$\frac{\mathrm{d}\Delta_\gamma}{\mathrm{d}E_\gamma} \Bigg/ \left(\frac{\mathrm{d}M_\gamma}{\mathrm{d}E_\gamma}\right)_{^{32}\mathrm{S}+^{58}\mathrm{Ni}} = \left[\left(\frac{\mathrm{d}M_\gamma}{\mathrm{d}E_\gamma}\right)^{\mathrm{dinucleus}}_{^{32}\mathrm{S}+^{64}\mathrm{Ni}} - \left(\frac{\mathrm{d}M_\gamma}{\mathrm{d}E_\gamma}\right)^{\mathrm{dinucleus}}_{^{32}\mathrm{S}+^{58}\mathrm{Ni}}\right] \Bigg/ \left(\frac{\mathrm{d}M_\gamma}{\mathrm{d}E_\gamma}\right)_{^{32}\mathrm{S}+^{58}\mathrm{Ni}}.$$

From the percent difference of fig. 4 it is clear that even after the subtraction of the complex fragment statistical γ-ray spectra from the data, there are still more γ-rays emitted in the more N/Z asymmetric reaction, *i.e.*, more γ-rays coming from the associated dinucleus.

The fact that the theoretical γ-ray multiplicities had to be divided by a factor of 1.8 to reproduce the experimental ones indicates that the total excitation energy shared among the fragments was too large. Indeed, according to different experimental findings [24,25] at the present incident energies there is some pre-equilibrium particle emission which has to be taken into account in the calculation of the total excitation energy.

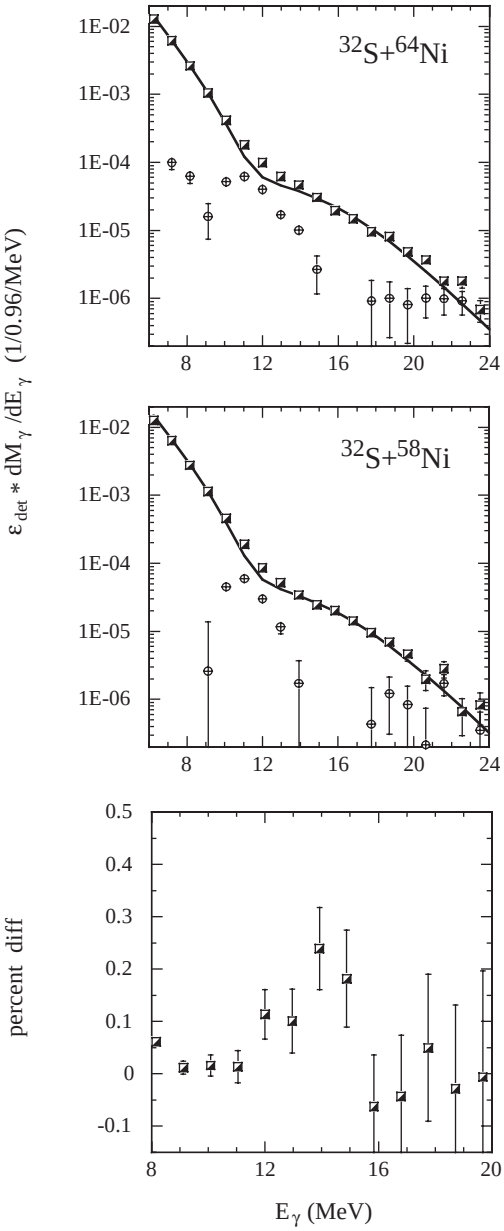

Fig. 5. The same as in fig. 4 in the hypothesis of pre-equilibrium emission of a proton and a neutron. In this hypothesis there is no normalization factor between data and calculations.

If we use the empirical relation given in ref. [25] the energy taken away from the emitted pre-equilibrium particles during the ^{32}S + ^{64}Ni and the ^{32}S + ^{58}Ni reaction is found to be $\Delta E = 29$ MeV and $\Delta E = 34$ MeV, respectively, by assuming the emission of one proton and one neutron. Then, the most probable initial fragmentations for the two reactions can be considered: ^{32}S + ^{62}Co and ^{32}S + ^{56}Co. The total excitation energy, lowered by the energy lost in the pre-equilibrium emission of 2 nucleons, by assuming always thermal equilibrium at the fragmentation moment, was shared between the primary fragments according to their masses. The corresponding excitation

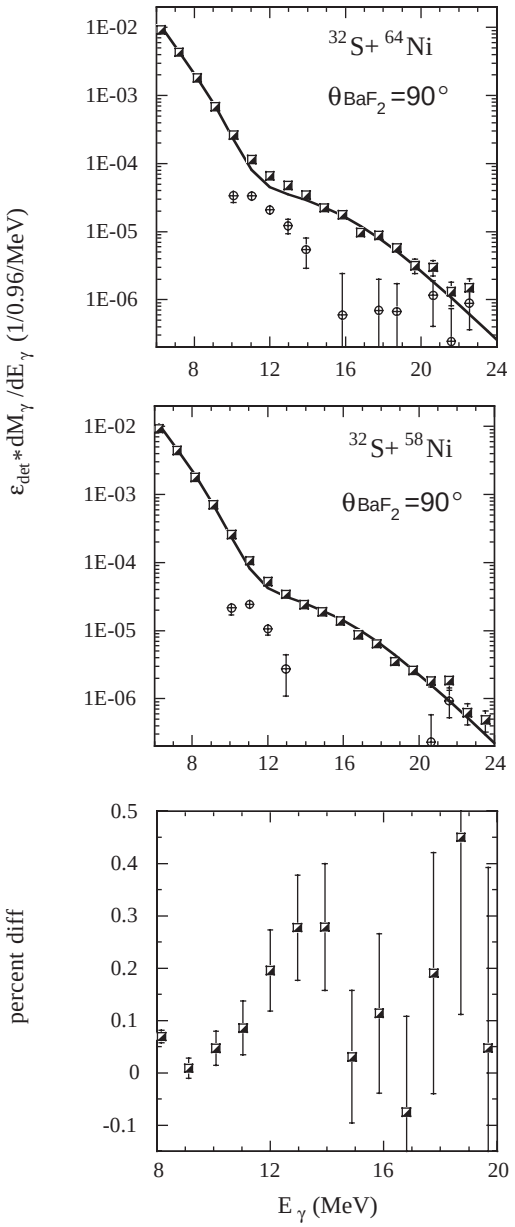

Fig. 6. The same as in fig. 5 for data obtained with BaF_2 scintillators situated at $\theta = 90°$ with respect to the beam direction.

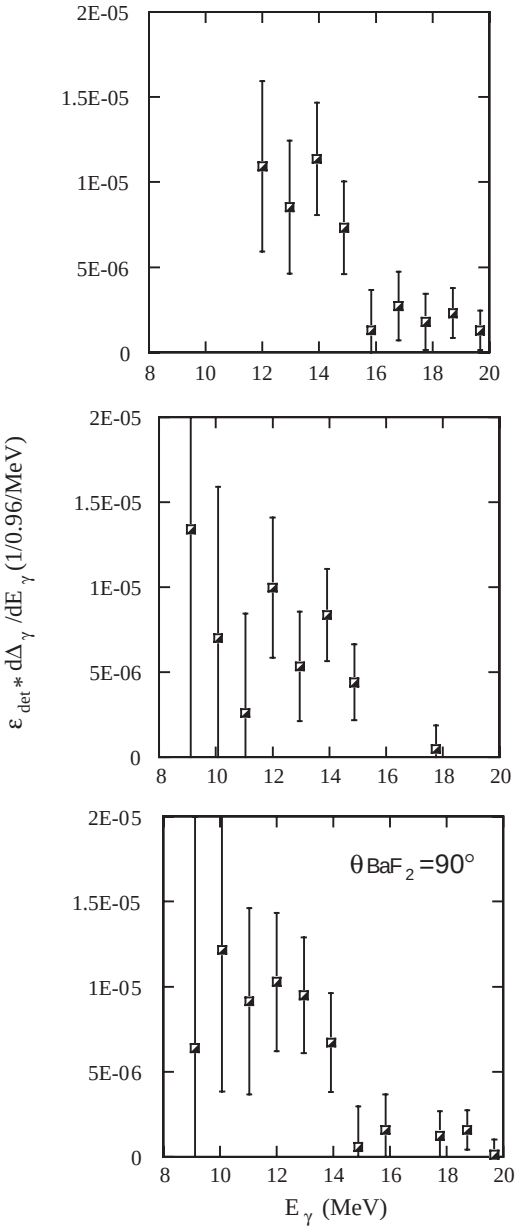

Fig. 7. Difference between the dinucleus γ-ray spectra associated with the ^{32}S + ^{64}Ni and ^{32}S + ^{58}Ni reaction in the laboratory reference frame by using the spectra (circles) of: upper panel: fig. 4; middle panel: fig. 5; lower panel: fig. 6.

energies and spins of the primary complex fragments are presented in table 2.

As previously, by using the code CASCADE, only the statistical γ-ray spectra for the most probable fragmentation were calculated, *i.e.* of S-like and Co-like fragments. The statistical model parameters used in the calculation are given in table 2.

The used GDR centroid energy for the target-like fragments, ^{56}Co and ^{62}Co, is in good agreement with the ground-state systematics concerning the ^{59}Co [19]. In this case as well, all the theoretical γ-ray spectra were folded with the experimental set-up response function and were corrected for the Doppler effect due to the velocity of the fragments.

By using the same symbols as in fig. 4, in fig. 5 the data and the theoretical spectra are presented. The theoretical spectra were obtained assuming a pre-equilibrium emission of 2 nucleons, therefore in the hypothesis of a lowered total excitation energy. The experimental γ-ray multiplicities are well reproduced by the theoretical ones at low and high energies both in shape and in absolute value without any normalization factor. However, also in this case, the theoretical γ-ray multiplicity is lower than the experimental one in the energy range from ∼10 to ∼18 MeV, the difference originating in the dinucleus γ-ray emission (circles in the upper and middle panel). The percent difference between the dinucleus γ-ray

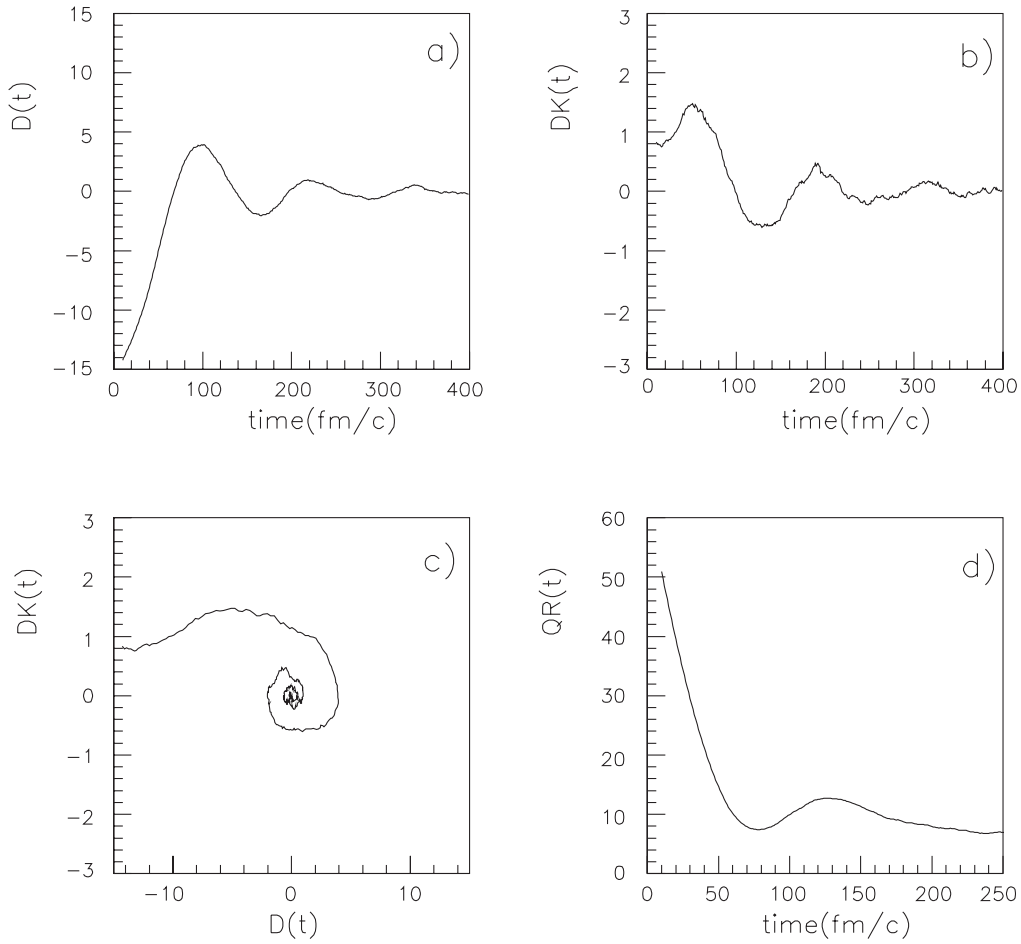

Fig. 8. System $^{32}S + ^{64}$ Ni at 10 A MeV. Impact parameter $b = 1$ fm, central collisions. Time evolution of: a) $D(t)$ (in fm units); b) $DK(t)$ (in fm^{-1}); c) $D(t)/DK(t)$ correlation; d) Mass quadrupole moment (in fm^2).

spectra associated with the two reactions is displayed in the lower panel of the same figure. Also here, more γ-rays are found to be emitted from the dinucleus during the reaction with the larger initial dipole moment.

It is worth noting that by taking into account the pre-equilibrium particle emission there is no need for normalization of the theoretical γ-ray multiplicities to the experimental ones. Therefore, the lowering of the total excitation energy caused from a pre-equilibrium light particle emission is necessary to reproduce both the shape and the absolute value of the data. In this hypothesis, the total excitation energy shared by the complex fragments is equal in the two reactions within the uncertainties of the model used for the calculation (see table 2).

It was also checked that by modifying the GDR parameters used in the CASCADE calculations within ± 0.5 MeV for the centroid energy, ± 2 MeV for the width and ± 0.1 for the dipole strength, the difference between the γ-ray emission of the dinucleus in the two reactions does not vanish.

In fig. 6 the cumulative experimental γ-ray spectra obtained with the BaF_2 scintillators situated at $\theta = 90°$ with respect to the beam direction are displayed for both reactions (squares) together with the calculated spectra for this specific angle and in the hypothesis of a pre-equilibrium emission of 2 nucleons (solid lines). The circles represent the dinucleus contribution in the two reactions. In the lower panel the percent difference between the dinucleus γ-ray spectra associated with the two reactions is presented.

From what was shown up to now, a larger emission of dipole γ-rays occurs during the more N/Z asymmetric deep-inelastic reaction which cannot originate in the γ-decay of the complex fragments. These dipole γ-rays in excess are emitted from the corresponding dinucleus before fragmentation.

In fig. 7 the difference between the γ-ray spectrum of the dinucleus created in the two reactions is presented in the two hypotheses for the calculation of the total excitation energy to be shared between the primary fragments. In the upper (middle) panel of fig. 7 the difference obtained without (with) pre-equilibrium particle emission is displayed for the two reactions. In the lower panel is reported the difference obtained with the BaF_2 scintillators situated at $\theta = 90°$ in the hypothesis of pre-equilibrium particle emission.

The difference $\varepsilon_{\rm det} * \frac{{\rm d}\Delta_\gamma}{{\rm d}E_\gamma}$ is attributed to the unequal initial dipole moment in the corresponding entrance

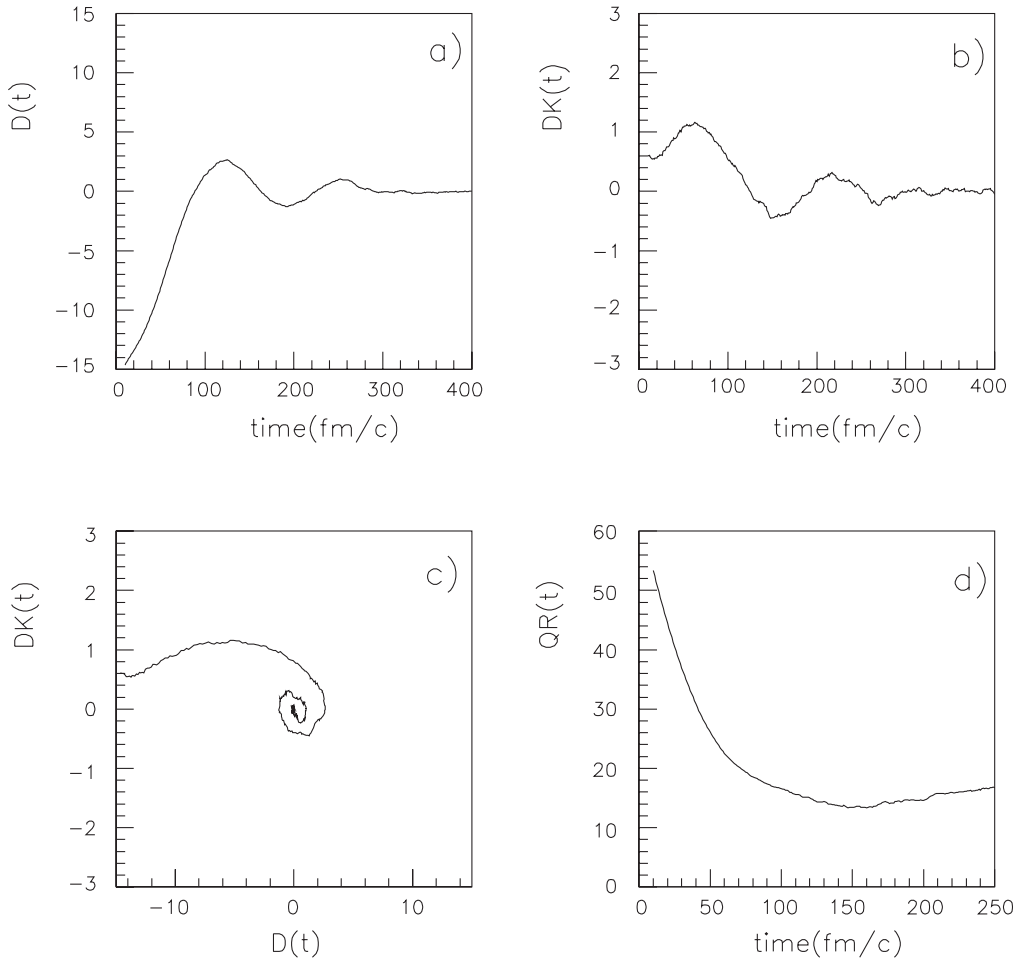

Fig. 9. Like previous figure. Impact parameter $b = 6$ fm, semiperipheral collisions.

channels. If $\varepsilon_{\rm det} * \frac{{\rm d}\Delta_\gamma}{{\rm d}E_\gamma}$ is integrated over the energy region between 10 and 20 MeV by taking into account the detector efficiency we obtain the energy integrated multiplicity of dinucleus dipole γ-rays caused by the initial dipole moment difference. We estimate $\Delta_\gamma \sim 1.4 \cdot 10^{-4}\gamma$ /decay for the upper panel and $\Delta_\gamma \sim 1.2 \cdot 10^{-4}\gamma$ /decay for the middle one.

Since in the hypothesis of pre-equilibrium particle emission both the shape and the absolute value of the experimental γ-ray multiplicity spectra are reproduced, in the following this hypothesis will be retained. All of the spectra in the previous figures are displayed in the laboratory reference frame. Then, in order to have the energy integrated dipole γ-ray multiplicity of the composite system in the reaction center-of-mass, the data and the calculated statistical γ-ray spectra of the fragments should be presented in the center of mass reference frame. Otherwise, one can consider the difference obtained only with the BaF_2 scintillators situated at $\theta = 90°$ (lower panel of fig. 7), where the Doppler-shift correction due to the velocity of the composite system is negligible. In that case, $\Delta_\gamma \sim 3 \cdot 10^{-4}\gamma$ /decay.

The energy integrated dipole γ-ray multiplicity of the dinucleus and that of the statistical part of the spectrum coming from the decay of the complex fragments in the two reactions, can be obtained by integrating the differential γ-ray multiplicity in the range $E_\gamma = 10$–20 MeV of the corresponding quantities for $\theta = 90°$ and by taking into account the detection efficiency.

In the case of the ^{32}S + ^{58}Ni reaction the energy integrated dipole γ-ray multiplicity of the dinucleus is $(3 \pm 1) \cdot 10^{-4}\gamma$ /decay, while that of the statistical part is equal to $(2.7 \pm 0.5) \cdot 10^{-3}\gamma$ /decay. In the case of the ^{32}S + ^{64}Ni reaction the energy integrated dipole γ-ray multiplicity of the dinucleus is $(5.6 \pm 1) \cdot 10^{-4}\gamma$ /decay, while that of the statistical part is equal to $(3 \pm 0.5) \cdot 10^{-3}\gamma$ /decay. Then, the ratio of the dinucleus/statistical part of the γ-ray spectrum is of the order of 10% for the ^{32}S + ^{58}Ni reaction and 20% for the ^{32}S + ^{64}Ni one.

The masses of the intermediate systems created during the two reactions differ by 6 nucleons. However, as we have already pointed out in the introduction, the dipole γ-ray emission of the dinucleus created in charge asymmetric peripheral heavy-ion collisions corresponds essentially to a dipole radiation during the charge equilibration process. This kind of radiation depends on the absolute value of charge which has to be shifted in order to restore the $(N_t + N_p)/(Z_t + Z_p)$ equilibrium ratio of the composite

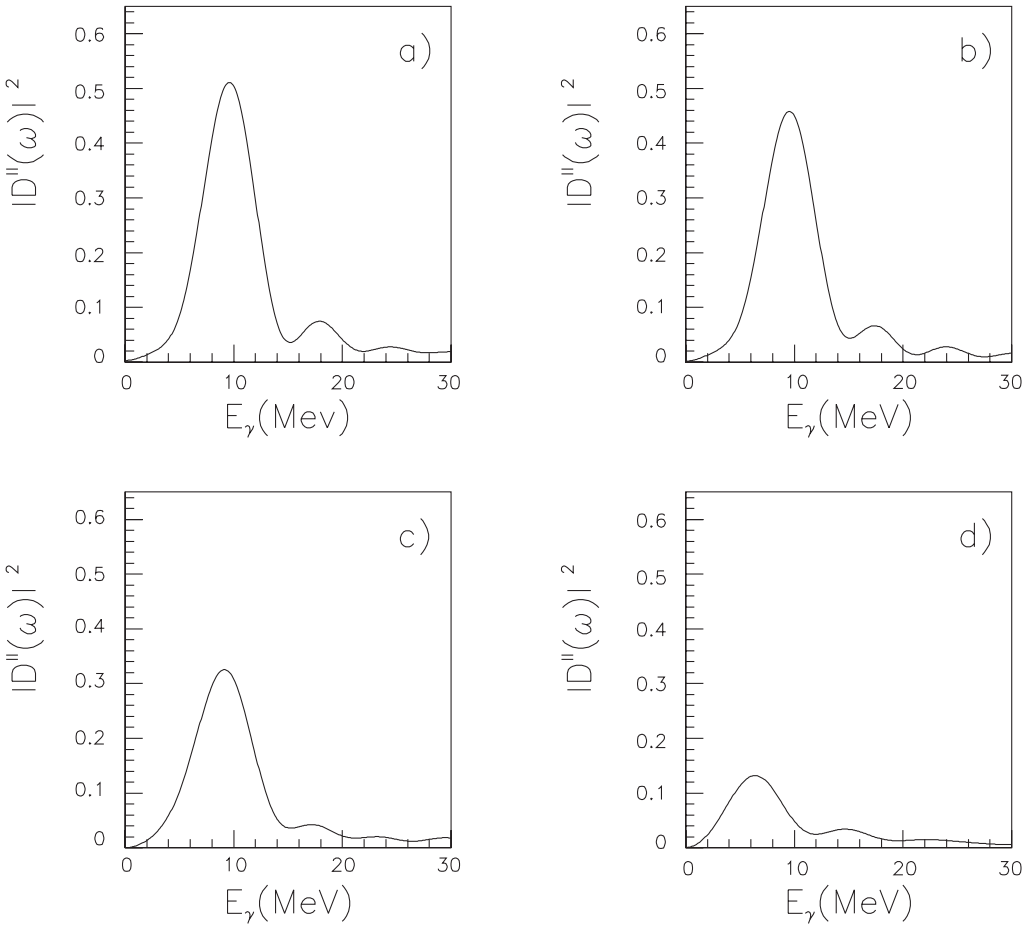

Fig. 10. System ^{32}S $+^{64}$ Ni at 10 A MeV. Power spectrum $|D''(\omega)|^2$ (in c^2 units): a) impact parameter $b = 1$ fm; b) $b = 3$ fm (fusion dominance, see text); c) $b = 5$ fm; d) $b = 7$ fm (deep-inelastic dominance).

system [13], therefore it should not be influenced by such a mass difference. We also note that the dinucleus dipole collective mass, NZ/A, is changing only by less than 10%. This quantity, through its square, is directly affecting the pre-equilibrium emission probability (see next section). So the net effect of the composite system mass difference can be neglected for the dynamical dipole discussion.

5 Discussion and theoretical predictions

The dynamics of dissipative reactions is described in a microscopic approach based on semiclassical transport equations, where mean field and two-body collisions are treated in a self-consistent way, see details in [3]. Realistic effective interactions of Skyrme type are used. The numerical accuracy of the transport code has been largely improved in order to have reliable results also at low energies, just above the threshold for fusion reactions [3,4,26]. The resulting physical picture is in good agreement with quantum Time-Dependent-Hartree-Fock calculation [14]. In particular we have studied in detail how a collective dipole oscillation develops in the entrance channel [4].

First, during the *approaching phase*, the two partners, overcoming the Coulomb barrier, still keep their own response. Then a *dinuclear phase* follows when the conversion of relative motion energy in thermal motion starts to take place, mainly due to nucleon exchange. The composite system is not thermally equilibrated and manifests, as a whole, a large amplitude dipole collective motion. Finally thermally equilibrated reaction products are formed, with consequent statistical particle/radiation emissions.

In the second *(dinuclear)* phase some pre-equilibrium collective dipole radiation can be also emitted. We can directly apply a Bremsstrahlung *("bremss")* approach [27, 15] to estimate this contribution.

The total photon emission probability from the dipole mode oscillations, as given by the Bremsstrahlung formula, can be expressed as [28] ($E_\gamma = \hbar\omega$)

$$\frac{\mathrm{d}P}{\mathrm{d}E_\gamma} = \frac{2e^2}{3\pi\hbar c^3 E_\gamma}\left(\frac{NZ}{A}\right)^2 |X''(\omega)|^2\,, \qquad (3)$$

where $X''(\omega)$ is the Fourier transform of the acceleration $X''(t)$ associated with the distance between the centers of mass of protons (P) and neutrons (N), $X = R_p - R_n$. $A = N + Z$ is the system mass. Thus, following the time evolution of the dipole mode along the fusion and deep-inelastic dynamics, it is possible to evaluate, in absolute values, the corresponding pre-equilibrium photon emission [15].

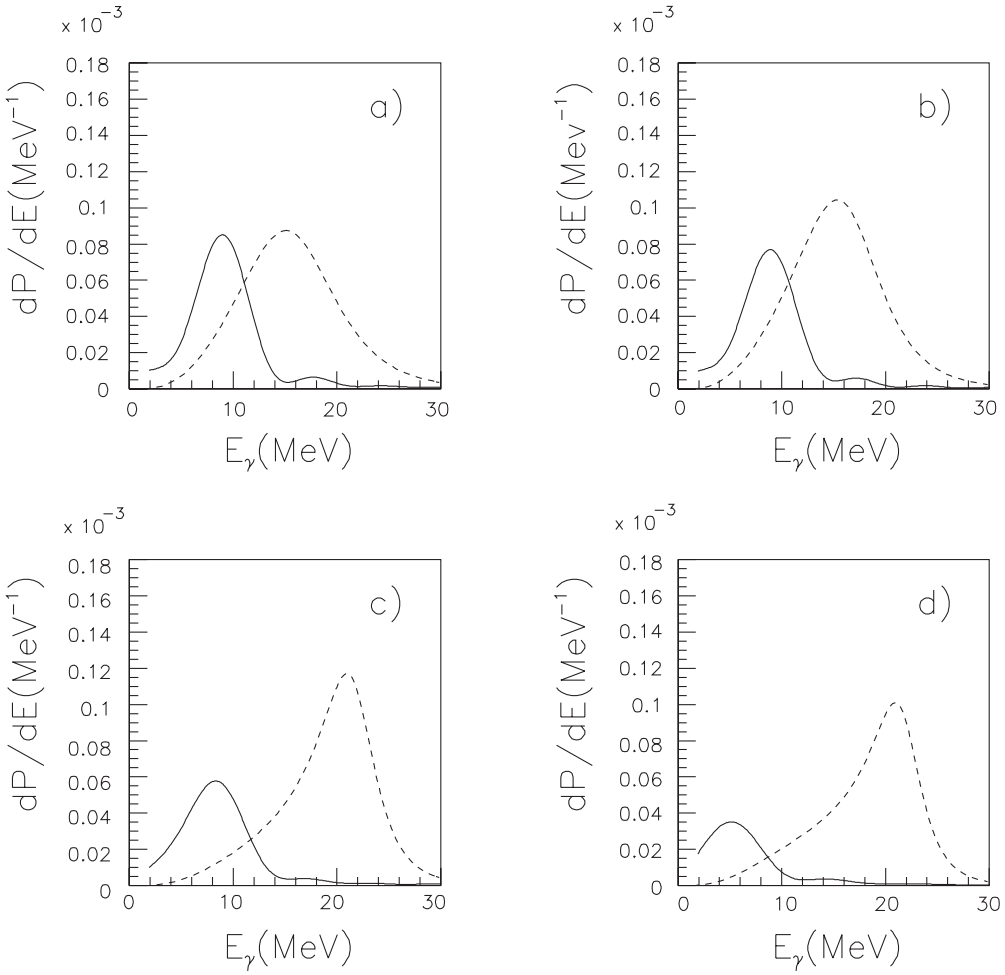

Fig. 11. System ^{32}S +^{64} Ni at 10 A MeV. Bremsstrahlung spectrum (solid lines) and the first-step statistical spectrum (dashed lines): a) impact parameter $b = 1$ fm; b) $b = 3$ fm (fusion dominance, see text); c) $b = 5$ fm; d) $b = 7$ fm (deep-inelastic dominance).

Now we focus on the dynamical dipole mode in the entrance channel and we study the dependence of the pre-equilibrium dipole oscillations on the centrality of the collision. We look at the relative weight *vs.* the statistical contribution.

We show results obtained from "*ab initio*" reaction simulations for the system ^{32}S($N/Z = 1$) on ^{64}Ni($N/Z = 1.28$), at 10A MeV, in order to compare with the present data [29].

From figs. 8, 9 we see how the dynamical dipole effect depends on the impact parameter and related main reaction mechanism, from $b = 1$ fm (fig. 8) where we have a fusion dominance to $b = 6$ fm (fig. 9) where we get mostly binary events. The plotted results represent an average over several simulation events.

Panels a),b) show the time evolution of the dipole moment in r-space, $D(t) = \frac{NZ}{A}X(t)$, and in p-space, $DK(t) = \Pi/\hbar$, where $\Pi = \frac{NZ}{A}(\frac{P_p}{Z} - \frac{P_n}{N})$, with P_p (P_n) center of mass in momentum space for protons (neutrons), is just the canonically conjugate momentum of the X coordinate, see [4,15]. We choose the origin of time at the beginning of the *dinuclear* phase. The nice "spiral" correlation in panel c) clearly denotes the collective nature of the mode. Finally in panel d) the mass quadrupole moment is reported, to indicate the main reaction process, from oscillations to fusion (fig. 8d) to separation in deep-inelastic collisions (fig. 9d).

From figs. 8, 9 we note that the "spiral-correlation" starts when the initial dipole moment $D(t = 0)$, the geometrical value at the touching point, is already largely quenched. This is the reason why the dinucleus dipole yield is not simply given by the "static" estimation but the reaction dynamics has a large influence on it. In any case in our simulations we have a much smaller collective dipole dinuclear excitation for the more charge symmetric system ^{32}S + ^{58}Ni, see [29]. Therefore, here we will focus our study on the new interesting impact parameter dependence of the pre-equilibrium dipole radiation for the system with larger entrance channel charge asymmetry.

From figs. 8, 9 we clearly see that the dynamical dipole is present even for dissipative binary collisions (deep inelastic) but the effect is decreasing with the centrality and the amount of dissipation. The latter point can be quantitatively estimated from the power spectrum, Fourier

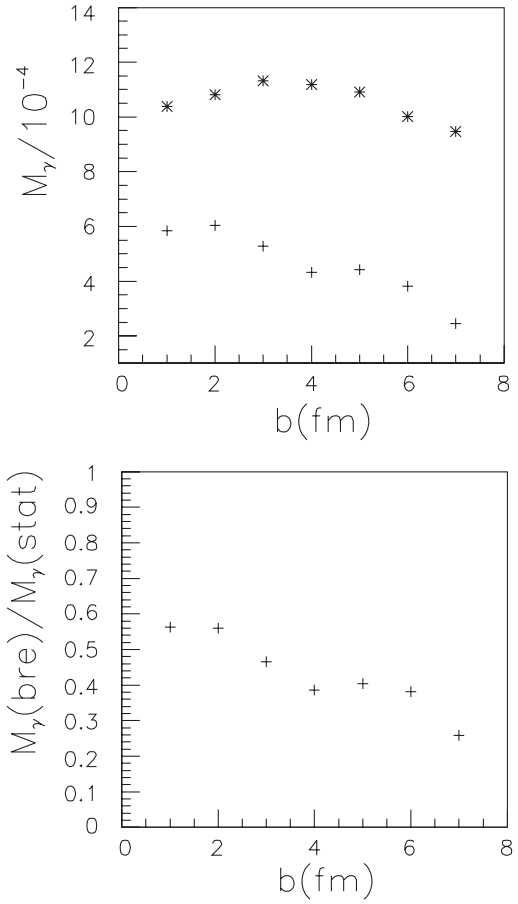

Fig. 12. System $^{32}S + ^{64}$Ni at 10 A MeV. Integrated photon multiplicities *vs.* centrality: Top: crosses, "*bremss*" contribution (dinucleus); stars, first-step statistical. Bottom: (bremss/stat) ratio.

transform of the dipole acceleration, plotted in fig. 10 for increasing impact parameters.

From the Bremsstrahlung formula eq. (3) this quantity directly gives the total photon emission probability from the pre-equilibrium dipole mode, which is reported in fig. 11.

In the same figure we show the first step statistical spectrum (dashed lines). The latter is just the product of the statistical γ-decay rate [30], times the mean lifetime of the equilibrated source [15]. The properties (masses and charges, excitation energies, angular momenta) of the primary hot sources (heavy residue or Projectile-like/Target-like fragments) are directly extracted from the simulation [29]. For the statistical GDR, the standard parameters from systematics, including temperature dependence of the width, are considered.

We note that, with increasing impact parameters, while the pre-equilibrium spectrum is shifted towards lower energies as a consequence of the larger dinuclear deformation, the statistical contribution is showing an opposite trend, since for binary events we have a thermal GDR emission from lighter systems.

Finally in fig. 12 we report the total photon multiplicities integrated over the two resonance regions (see fig. 11), of the dynamical dipole (crosses) and of the statistical GDR (stars), respectively. In the same fig. 12 (bottom) we present also the ratio between total pre-equilibrium and total statistical (first step) multiplicities.

We remark that this calculation is completely parameter-free and no normalization to data is performed. The results are clearly showing the dynamical dipole emission in deep-inelastic reactions with charge asymmetry in the entrance channel. Moreover we see an appreciable agreement with the data for the absolute value of the integrated "dinucleus" multiplicity, fig. 12 (top), as well as for the ratio to the statistical part, of the order of 30–40% in the deep-inelastic case. This is actually somewhat larger than experiments, but only first-step statistical decays are considered.

6 Conclusions

In this work the dependence of the pre-equilibrium dipole γ-ray emission on the entrance channel charge asymmetry in the $^{32}S + ^{58}$Ni and $^{32}S + ^{64}$Ni peripheral collisions has been investigated. In these reactions, apart the entrance channel charge asymmetry, the other relevant parameters were kept constant. The energy spectra of the γ-rays detected in coincidence with the complex fragments emitted in the two reactions were compared with each other for fast quasi-elastic and slower deep-inelastic collisions. For quasi-elastic collisions the differential γ-ray multiplicity for the two reactions was identical within the error bars in the whole energy region of interest, while for deep-inelastic collisions a difference appears in the energy range $E_\gamma = 10$–16 MeV with the more N/Z asymmetric reaction having the larger differential γ-ray multiplicity.

In order to isolate the dinuclear system contribution in the total experimental γ-ray spectrum, calculations were performed within the statistical model to evaluate the theoretical γ-ray spectrum originating in the statistical decay of the primary complex fragments emitted during the reactions. The difference was still present in the same energy range after the theoretical γ-ray spectra of the fragments were subtracted from the experimental ones. According to the conclusion drawn throughout the paper, this difference comes from a larger dipole γ-ray emission from the dinucleus created during the more N/Z asymmetric collision. The absence of any difference between the data for quasi-elastic events was associated with the short dinucleus lifetime, as fragmentation occurs before complete relaxation of the charge degree of freedom between the colliding ions.

The theoretical analyses based on a collective Bremsstrahlung approach [15] are qualitatively *and* quantitatively confirming the presence of a prompt dipole radiation for the charge asymmetric system in *all* dissipative collisions, from fusion to deep inelastic. For that system, a good agreement is obtained between the theoretical absolute value of the energy integrated dinucleus dipole γ-ray multiplicity for an impact parameter $b \sim 6$ fm (see fig. 12 (top)) and the experimental one.

The collective dinuclear dipole emission is decreasing with the centrality of the collision (see fig. 12) and therefore with the kinetic energy loss. This is not surprising since the same mean-field dynamics is behind both effects, dissipation and collective dipole mode. For very peripheral reactions the dynamical radiation is rapidly disappearing since the interacting system has no time to "organize" a dinuclear mean field before separation.

Recently, a dependence of the prompt dipole γ-ray emission on the incident energy was predicted [4,15] and a range of incident energies was found, where the N/Z effect becomes stronger. In the future, exotic beams could be of great interest for the study of the dynamical dipole excitation both on the entrance channel charge asymmetry and on the incident energy by allowing to obtain large entrance channel charge asymmetries. Since the prompt dipole γ-ray emission is a cooling mechanism of the composite system in fusion reactions its systematic study could be a significant aid in the superheavy-element formation.

The authors would like to thank A. Vitturi and P. F. Bortignon for stimulating discussions.

References

1. Ph. Chomaz, M. Di Toro, A. Smerzi, Nucl. Phys. A **563**, 509 (1993)
2. P.F. Bortignon *et al.*, Nucl. Phys. A **583**, 101c (1995).
3. V. Baran *et al.*, Nucl. Phys. A **600**, 111 (1996).
4. V. Baran *et al.*, Nucl. Phys. A **679**, 373 (2001).
5. S. Flibotte *et al.*, Phys. Rev. Lett. **77**, 1448 (1996).
6. M. Cinausero *et al.*, Nuovo Cimento **111**, 613 (1998).
7. D. Pierroutsakou *et al.*, Nucl. Phys. A **687**, 245c (2001); to be published in Eur. Phys. J. A.
8. L. Campajola *et al.*, Z. Phys. A **352**, 421 (1995).
9. M. Sandoli *et al.*, Z. Phys. A **357**, 67 (1997).
10. M. Sandoli *et al.*, Eur. Phys. J. A **6**, 275 (1999).
11. M. La Commara *et al.*, *Proceedings of the XXXIV International Winter Meeting on Nuclear Physics, Bormio 1996*, edited by I. Iori (Dipartimento di Fisica, Università degli Studi di Milano, 1996) p. 394.
12. M. Papa *et al.*, Eur. Phys. J A **4**, 69 (1999).
13. C.H. Dasso, H. Sofia, A. Vitturi, Eur. Phys. J. A **12**, 279 (2001).
14. C. Simenel *et al.*, Phys. Rev. Lett. **86**, 2971 (2000).
15. V. Baran, D.M. Brink, M. Colonna, M. Di Toro, Phys. Rev. Lett. **87**, 182501 (2001).
16. M. Trotta *et al.*, *Proceedings of the NUCOLEX99*, Riken Review No. 23, edited by N. Dinh Dang, U. Garg, S. Yamaji (1999) p. 96.
17. L. Campajola *et al.*, Nucl. Instrum. Methods A **342**, 534 (1994).
18. F. Puhlhofer, Nucl. Phys. A **280**, 27 (1977); M.N. Harakeh, extended version (private communication)
19. S.C. Fultz *et al.*, Phys. Rev. C **10**, 608 (1974); S.S. Dietrich, B.L. Berman, At. Data Nucl. Data Tables **38**, 199.
20. M. Kicinska-Habior *et al.*, Phys. Rev. C **36**, 612 (1987).
21. G. Viesti *et al.*, Phys. Rev. C **40**, R1570 (1989).
22. R. Brun *et al.*, CERN Report No. CERN-DD/EE/84-1 (unpublished, 1986).
23. H. Nifenecker, J. A. Pinston, Annu. Rev. Nucl. Part. Sci. **44**, 113 (1990).
24. B. Natowitz *et al.*, Z. Phys. A **325**, 467 (1986).
25. M.P. Kelly *et al.*, Phys. Rev. Lett. **82**, 3404 (1999).
26. M. Cabibbo *et al.*, Nucl. Phys. A **637**, 374 (1998).
27. A Bremsstrahlung approach, T. Papenbrock, G.F. Bertsch, Phys. Rev. Lett. **80** 4141 (1998) was applied to calculate the photon emission during the alpha-decay process. In our calculations the classical *"bremss"* appears justified since the dynamics is well above the threshold and so in a classical allowed region.
28. J.D. Jackson, *Classical Electrodynamics* (Wiley, New York, 1962).
29. N. Pellegriti, Diploma Thesis, University of Catania, 2002.
30. K.A. Snover, Annu. Rev. Nucl. Part. Sci. **36**, 545 (1986).